Bull. Chem. Soc. Jpn., 71, 17—29 (1998)

Accounts

Reduction of CO_2 Directed toward Carbon–Carbon Bond Formation

Koji Tanaka

Institute for Molecular Science, Myodaiji, Okazaki 444

(Received June 12, 1997)

This paper describes electrochemical reduction of CO_2 directed toward carbon–carbon bond formation via metal–CO_2 adducts. An electrophilic attack of CO_2 to penta-coordinated low valent polypyridyl Ru complexes affords a Ru–η^1-CO_2 adduct, which is easily converted to Ru–CO species either by an acid-base equilibrium in protic media and oxide transfer to CO_2 under aprotic conditions. Two-electron reduction of resultant Ru–CO in protic solutions competitively causes a cleavage of the Ru–CO bond (CO evolution) and formation of a thermally labile Ru–CHO bond. Besides further reduction of the latter to Ru–CH_2OH as precursors to CH_3OH and $HOOCCH_2OH$, Ru–CHO reacts with CO_2 to afford HCOOH with regenerating Ru–CO as the precursor to CO. Thus, the difficulty of multi-electron reduction of CO_2 in protic solutions is ascribed to the thermal lability and strong hydride donor character of Ru–CHO. On the other hand, two-electron reduction of Ru–CO in the presence of $(CH_3)_4N^+$ or CH_3I under aprotic conditions produces thermally stable R–$C(O)CH_3$, which works as a precursor to $CH_3C(O)CH_3$. Two-electron reduction of $M_3(\mu_3\text{-}S)_2$ clusters (M = Co, Rh, Ir) causes an M–M bond cleavage and the nucleophilicity of the μ_3-S ligand is also enhanced. As a result, two CO_2 molecules reductively activated probably on μ_3-S and metal sites undergo the coupling reaction to give oxalate selectively.

Much attention has been paid to the utilization of CO_2 as a C1 source for chemicals and fuels to cope with an increase in the concentration in air and the oil shortage predicted for the near future. Carbon dioxide behaves as an electrophile under normal conditions. It is well known that CO_2 smoothly inserts into metal–alkyl and –aryl (M–R) bonds to form the corresponding M–OC(O)R complexes as precursors to carboxylic acids.[1] Dienes and alkynes coordinated to metals are also likely to undergo an electrophilic attack of CO_2 to give lactones and pyrones.[2] In contrast to such electrophilic attack of CO_2 to organic substrates activated on metals, incorporation of CO_2 activated on metals to relatively inert organic substrates still remains unusual in organic syntheses. Carbon dioxide usually binds to low valent of metals with an η^1- or η^2-mode, where the electron density of the CO_2 group is greatly enhanced due to back electron transfer from the metal to CO_2. The η^1-CO_2 mode is composed of electron transfer from the filled d_z2 orbital of d^8 metal centers to the CO_2 π^* orbital, and the η^2-CO_2 mode involves electron transfer from a filled CO_2 π to metal in addition to that from a filled metal πd to the empty CO_2 π^* orbital. The first metal CO_2 complex (M–CO_2) was $Ni(PCy_3)_2(\eta^2\text{-}CO_2)$ prepared by Aresta et al. in 1975.[3] Since then, a variety of metal complexes with η^1-η^2-,μ^2-, and μ^3-CO_2 modes have been prepared.[4] Most M–η^1-CO_2 complexes are thermally labile and are easily oxidized by air. A C–O bond of M–η^1-CO_2 complexes is easily cleaved either by protonation in protic media or by oxide transfer to free CO_2 in aprotic media, while such transformation from M–η^2-CO_2 to M–CO has not been demonstrated so far. Accordingly, CO evolution in electro- and photochemical reduction of CO_2 catalyzed by metal complexes has been simply explained by M–η^1-CO_2 intermediates, but little direct evidence has been obtained. One of the most crucial problems in electro- and photochemical reduction of CO_2 using homogeneous catalysts is why the products are limited to only CO and/or HCOOH.[5] Elucidation of the problem would greatly contribute to constructing a catalytic system that enables multi-electron reduction of CO_2 with forming new carbon–carbon bonds near the equilibrium potentials of the reactions.

A key question for the formation of M–η^1-CO_2 complexes how to create coordinatively unsaturated low valent metal centers under mild conditions. On the other hand, adduct formation between CO_2 and organic bases is generally much easier than the formation of M–η^1-CO_2 ones. The OCO angle of both adducts probably depends on the number of electrons transferred to the CO_2 moieties. The linear OCO of free CO_2 is hardly influenced at all by adduct formation with a weak base such as NH_3CO_2. On the other hand, the OCO angle of the imidazolidone–CO_2 adduct ($OOC\text{–}\overline{NC(O)\text{-}NHCH_2CH_2}\overline{)}^-$ is calculated as 132°,[6] which is quite close to those of [Co(Pr-salen)K(η^1-CO_2)] (132°) and [Rh(diars)-

2(η^1-CO_2)] (126°).[7] Thus, CO_2 bonded to strong organic bases is also reductively activated similar to the process on low valent metals. A fundamental difference in the reductive activation of CO_2 on metals and organic bases is that the CO_2/CO conversion takes place on the former, but practically does not on the latter. Reductive activation of CO_2 on organic bases, therefore, may be utilized in CO_2 fixation without any accompanying C–O bond cleavage. It is worthy of note that acidity and basicity of neighboring groups (ligands) of the central metals are largely influenced by redox reactions of metal complexes even if the reactions are simply explained by the change of oxidation numbers of the central metals. Accordingly, basic ligands as well as metals are possible binding sites for the reductive activation of CO_2, and the reactivity of the activated CO_2 on both sites are regulated by the redox reaction of the metal complexes.

This article focuses on activation of CO_2 on metals and ligands directed toward multi-electron reduction of CO_2 accompanied by carbon–carbon bond formation in the electrochemical reduction of CO_2 catalyzed by metal complexes.

Metal–η^1-CO_2 Complexes

The first M–η^1-CO_2 (M = transition metal) complex was prepared by the reaction of CO_2 with [Co^I(salen)M]$^+$ (M=Li, Na, K, and Cs), where alkali metals used for the reduction of [Co^{II}(salen)] remains in the Co–η^1-CO_2 adducts and strongly interacts with oxygen of CO_2 binding to Co(I) (Eq. 1).[7a]

$$[Co^I(salen)M]^+ + CO_2 \longrightarrow [Co^I(salen)M(CO_2)]^+ \quad (1)$$

Since then, a series of the Co^I–η^1-CO_2 complexes with Shiff bases and macrocyclic ligands have been characterized.[8] The electron donor ability of the central metal atoms gives crucial influences on the stability of the M–η^1-CO_2 bond. In fact, Co(I) complexes with the redox potential of the Co(I)/Co(II) couple more positive than −1.2 V essentially lose the ability to bind CO_2 at room temperature.[9] Similar to Co^I–η^1-CO_2 complexes, anionic [CpM$(CO)_2(\eta^1$-$CO_2)]^-$ (M=Fe, Ru)[10] and [$W(CO)_5(\eta^1$-$CO_2)]^{2-}$ [11] were prepared by the reaction of [CpM$(CO)_2]^-$ and [$W(CO)_5]^{2-}$ with CO_2 at low temperatures. Neutral Rh- and Ir–η^1-CO_2 complexes are prepared by an electrophilic attack of CO_2 to penta-coordinated [Ir^ICl-(dmpe)$_2$][12] and [Rh^ICl(diars)$_2$].[7b] Another synthetic route for M–η^1-CO_2 complexes is deprotonation of M–C(O)OH complexes derived from a nucleophilic attack of OH^- (or H_2O) to carbonyl carbon of electron deficient M–CO complexes (Eq. 2).

$$[M\text{–}CO]^{(n+2)+} \underset{-OH^-}{\overset{OH^-}{\rightleftharpoons}} [M\text{–}C(O)OH]^{(n+1)+} \underset{-OH^-}{\overset{OH^-}{\rightleftharpoons}} [M\text{–}CO_2]^{n+} + H_2O \quad (2)$$

As M–η^1-CO_2 complexes are generally not stable in H_2O, only a series of [Ru$(bpy)_2(CO)(\eta^1$-$CO_2)$], [Ru-$(bpy)_2(CO)${C(O)OH}]$^+$, and [$Ru(bpy)_2(CO)_2]^{2+}$ have been shown to exist as equilibrium mixtures in H_2O (see below).[13] A general tendency for the relative stability of M–C(O)OH and M–η^1-CO_2 complexes is not clear, because [FeCp$(PPh_3)(CO)${C(O)OH}] loses CO_2 faster than [FeCp-$(PPh_3)(CO)(\eta^1$-$CO_2)]^-$,[14] but the reverse is true for [ReCp-$(NO)(CO)${C(O)OH}]$^-$[15] and [$IrCl_2(PMe_2Ph)_2(CO)${C(O)-OH}].[16] The basicity of an η^1-CO_2 group, that has a fundamental importance to understand the reactivity of the M–η^1-CO_2 complexes, can be reasonably evaluated from the conjugated acids, M–C(O)OH complexes. In contrast to pK_a values of organic carboxylic acids, the values of M–C(O)OH complexes widely range from ca. 2 to over 14 (Table 1) due to a large difference in the electron donor ability of the central metals to the CO_2 group. Despite such large differences in the basicity of M–η^1-CO_2 complexes, the knowledge concerning the structures and the basicity of η^1-CO_2 group is quite limited, since only three M–η^1-CO_2 complexes have had their molecular structures determined X-ray analysis so far. The electronic states of M–η^1-CO_2 complexes would be represented by resonance forms of I, II, and III (Eq. 3).

$$\underset{\mathbf{I}}{M^{n+}\text{–}CO_2} \rightleftharpoons \underset{\mathbf{II}}{M^{(n+1)+}\text{–}CO_2^-} \rightleftharpoons \underset{\mathbf{III}}{M^{(n+2)+}\text{–}CO_2^{2-}} \quad (3)$$

The amounts of electrons transferred to CO_2 increased in the order I<II<III, and the M–CO_2 bond will be strengthened in the same order. The alkaline metal (M′) as a counter ion of [Co^I(salen)M′(η^1-CO_2)]$^+$ (Eq. 1) which strongly interacts with oxygen of the CO_2 group must assist the electron flow from Co^I to CO_2 to stabilize the Co–η^1-CO_2 bond.

An addition of 2 equiv of OH^- to an H_2O/CH_3OH solution of [$RuL_2(CO)_2]^{2+}$ (L=2,2′−bipyridine) crystallizes red [$RuL_2(CO)(\eta^1$-$CO_2)$]·3H_2O; this complex is exceptionally stable among those metal–η^1-CO_2 complexes reported so far. The interconversion among *cis*-[$RuL_2(CO)_2]^{2+}$, *cis*-[$RuL_2(CO)${C(O)OH}]$^+$ and *cis*-[$RuL_2(CO)(\eta^1$-$CO_2)$] in H_2O is very rapid (Eq. 4) and pK_a of [$RuL_2(CO)${C(O)-OH}]$^+$ is determined as 9.6 at 20 °C.[13]

$$[RuL_2(CO)_2]^{2+} \underset{-OH^-}{\overset{OH^-}{\rightleftharpoons}} [RuL_2(CO)\{C(O)OH\}]^+ \underset{H^+}{\overset{OH^-}{\rightleftharpoons}} [RuL_2(CO)(\eta^1 - CO_2)] \quad (4)$$

Molecular structures of the three complexes are determined by X-ray analysis.[17,18] The framework of the *trans*-N–Ru–CO, *trans*-N–Ru–C(O)OH, and *trans*-N–Ru–CO_2 moieties of [$RuL_2(CO)_2$](PF_6)$_2$, [$RuL_2(CO)$(C(O)OH)]-(H_2O)CF_3COO, and [$RuL_2(CO)(\eta^1$-$CO_2)$]·3H_2O, respectively, are depicted in Fig. 1. Red crystals of [$RuL_2(CO)(\eta^1$-$CO_2)$]·3H_2O contain three-dimensional hydrogen bonding

Table 1. pK_a Values of Hydroxycarbonyl Metal Complexes

Complex	pK_a	Ref.
ReCp(NO)(CO)(CO_2H)	11	15
[$RuL_2(CO)(CO_2H)]^+$	9.6	13
Pt(C_6H_5)(PEt_3)(CO_2H)	14	19
[$CoL(CO_2H)]^{2+}$	3.1	8d
[$Co(en)_2(H_2O)(CO_2H)]^{2+}$	2.5	8e

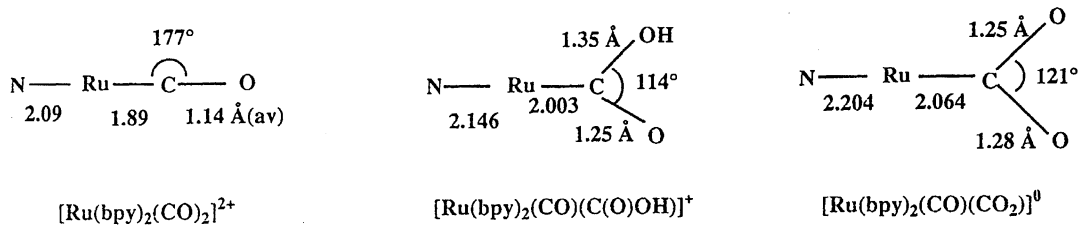

$[Ru(bpy)_2(CO)_2]^{2+}$ $[Ru(bpy)_2(CO)(C(O)OH)]^{+}$ $[Ru(bpy)_2(CO)(CO_2)]^{0}$

Fig. 1. *trans*-N–Ru–C frameworks of $[RuL_2X(CO)]^{2+}$, $[RuL_2X(C(O)OH)]^{+}$, and $[RuL_2X(CO_2)]$ (L=bpy; X=CO).

networks among two oxygens of the η^1-CO_2 ligand and three hydrate molecules, which must assist electron flow to the CO_2 group from Ru and stabilizes the Ru–CO_2 bond. Nonequivalent two C–O bond distances (1.25 and 1.28 Å) of the η^1-CO_2 group, therefore, are caused by the differences in the number of hydrogen bondings between the two oxygen and hydrate water molecules. The Ru–CO_2 bond distance (2.06 Å) is close to that of $[RhCl(diars)_2(\eta^1\text{-}CO_2)]$ (2.05 Å)[7b] but longer than of $[Co(Pr\text{-}salen)(K)(\eta^1\text{-}CO_2)]$ (1.99 Å).[7a] The average of the C–O bond distance in the η^1-CO_2 group (1.27 Å) is somewhat longer than the average of the C–O ones (1.23 Å) of $[RhCl(diars)_2(\eta^1\text{-}CO_2)]$ and $[Co(Pr\text{-}salen)(K)(\eta^1\text{-}CO_2)]$. The OCO angle (121°) of the Ru–CO_2 group is narrower than those of Rh–η^1-CO_2 (126°) and Co–η^1-CO_2 (135°). The C–O bond distance and the OCO angle of CO_2^- are calculated as 1.24 Å and 135.2°, respectively, by ab initio MO calculations.[19] If an OCO angle of metal–η^1-CO_2 complexes is correlated with the amount of electrons transferred to the CO_2 ligands, σ-donation from Ru to CO_2 is stronger than that from Co and Rh to CO_2. Based on the pK_a values of Ru–C(O)OH (9.6) and Co–η^1-C(O)OH complexes (2—3) (Table 1), and the OCO angles of $[RuL_2(CO)(\eta^1\text{-}CO_2)]$ (121°), $[Co(Pr\text{-}salen)(K)(\eta^1\text{-}CO_2)]$ (135°),[17] and CO_2^- (135°), the electronic states of the Ru– and Co–η^1-CO_2 complexes are approximated by the resonance forms III and II, respectively. Accordingly, $[RhCl(diars)_2(\eta^1\text{-}CO_2)$[7b] may be expressed by an intermediate between the resonance forms II and III on the basis of the OCO angle, though the pK_a value of the conjugated acid is not clear.

The relatively high electron density on the CO_2 group of $[RuL_2(CO)(\eta^1\text{-}CO_2)]$ is responsible for the smooth transformation from CO_2 to CO on the Ru atom in H_2O. The C=O and C–O bond distances (1.242 and 1.345 Å) and the OCO angle of 119° of $[RuL_2(CO)(C(O)OH)]^+$ are close to the values of $[Pt(C_6H_5)(PEt_3)_2\{C(O)OH\}]$,[19] which exists as a hydrogen-bonded dimer structure similar to the solid state of acetic acid. Protonation of the CO_2 group of $[RuL_2(CO)(\eta^1\text{-}CO_2)]$ causes shortening both the Ru–η^1-CO_2 and the Ru–N (*trans* to Ru–CO_2) bonds. Dehydroxylation of $[RuL_2(CO)\{C(O)OH\}]^+$ further shortens the Ru–C and Ru–N (*trans* to Ru–C(O)OH) bonds (Fig. 1). The Ru–η^1-CO_2 bond is primarily composed of σ-donation from Ru to CO_2, and the Ru–CO bond consists of π-back donation from Ru to CO and weak σ-donation from CO to Ru. The gradual elongation of the Ru-C bond distances from Ru–CO, Ru–C(O)OH to Ru–CO_2, therefore, strongly reflects the decrease in the π-bonding rather than the increase in the σ-bonding in the Ru–C bonds. It is worthy of note that an increase in the σ-donation from metals to CO_2 strengthens M–η^1-CO_2 bonds, but does not always shorten the Ru–C bond distances. The agreement of the order of the Ru–CO<Ru–C(O)OH<Ru–CO_2 bond distances with *trans*-Ru–N ones strongly indicates that bpy as a σ-donor and π-acceptor ligand plays a role as an electron reservoir in the serious changes in the electronic structures of Ru in the equilibrium of Eq. 4. It should be noticed that $[RuL_2(CO)(\eta^1\text{-}CO_2)]$ does not undergo a serious change at 100 °C in H_2O at pH 11 for 3 h, while $[CpRu(CO)_2(\eta^1\text{-}CO_2)]Na$ decomposes to $[CpRu(CO)_2(H)]$ in THF at 0 °C.[20] Thus, bpy ligands greatly contribute to the exceptional thermal stability of $[RuL_2(CO)(\eta^1\text{-}CO_2)]$ as a metal–η^1-CO_2 complex.

Conversion from M–CO_2 to M–CO under Aprotic Conditions

Anionic $[CpFe(CO)_2(\eta^1\text{-}CO_2)]^-$ and $[W(CO)_5(\eta^1\text{-}CO_2)]^{2-}$ smoothly react with CO_2 to produce $[CpFe^I(CO)_3]^+$ and $[W^0(CO)_6]$, respectively, with forming CO_3^{2-} (Eqs. 5 and 6).[20a,20b]

$$[W(CO)_5(\eta^1 - CO_2)]^{2-} + CO_2 \longrightarrow W(CO)_6 + CO_3^{2-} \quad (5)$$

$$[CpFe(CO)_2(\eta^1 - CO_2)]^{2-} + CO_2 \longrightarrow [CpFe(CO)_3]^+ + CO_3^{2-} \quad (6)$$

Thus, $[M\text{–}\eta^1\text{-}CO_2]^{n+}$ with a very strong basic CO_2 group undergoes the oxide transfer reaction by free CO_2 to generate CO_3^{2-} and $[M\text{–}CO]^{(n+2)+}$, the latter of which works as the precursor to CO in electrochemical reduction of CO_2 (reductive disproportionation of CO_2) under aprotic conditions (Eq. 7).

$$2CO_2 + 2e^- \longrightarrow CO + CO_3^{2-} \quad (7)$$

But no oxide transfer reaction from CO_3^{2-} to M–CO complexes (reverse reaction of Eqs. 5 and 6) has been reported so far. Comparison of the basicity of M–η^1-CO_2 and CO_3^{2-} as oxide donors would greatly help us to understand the differences in the two bonds on the basis of pK_a values of the conjugated acids: $[Ru(bpy)_2(CO)\{C(O)OH\}]^+$ (9.6)[7] and $HOCO_2^-$ (10.3).[22] Red crystals of $[RuL_2(CO)(\eta^1\text{-}CO_2)]\cdot 3H_2O$ are soluble only in protic media such as H_2O, CH_3OH, C_2H_5OH, but are insoluble in aprotic solvents. The characteristic solubility of the red crystals in both media is explained by the three dimensional hydrogen bonding networks of solvated water molecules in the solid state. On the other hand, the red crystals are smoothly solubilized into a CH_3CN solution containing $LiCF_3SO_3$ due to destruction of 3-dimensional hydrogen bonding networks of $[RuL(CO)(CO_2)]\cdot 3H_2O$ by interaction of Li^+ with oxygens of the η^1-CO_2 group.

The IR spectrum of a CD_3CN solution containing [RuL(CO)(CO_2)]·3H_2O and 3 equiv of $LiCF_3SO_3$ showed strong $\nu_{asym}(CO_2)$ and $\nu_{sym}(CO_2)$ bands at 1467 and 1246 cm^{-1}, which are close those of [$RuL_2(CO)(\eta^1\text{-}CO_2)$]·3$H_2O$ in KBr disks (1428 and 1242 cm^{-1}).[17] Thus, the molecular structure of [$RuL_2(CO)(\eta^1\text{-}CO_2)$]·3$H_2O$ in the solid state is maintained also in CH_3CN containing $LiCF_3SO_3$. Solubilization of [$RuL_2(CO)(\eta^1\text{-}CO_2)$] in aprotic media enabled the direct interconversion between [$RuL_2(CO)(\eta^1CO_2)$] and [$RuL_2(CO)_2$]$^{2+}$ without passing through [$RuL_2(CO)${C(O)OH}]$^+$. Similarly, we found that [$RuL_2(CO)(\eta^1\text{-}CO_2)$] is solubilized in CH_3CN in the presence of [K(crown)]$^+$.

The reaction of [K(crown)]$_2CO_3$ with [$RuL_2(CO)_2$]$(PF_6)_2$ afforded [$RuL_2(CO)(\eta^1\text{-}CO_2)$] and CO_2 in CH_3CN (Eq. 8).[21]

$$[Ru(bpy)_2(CO)_2]^{2+} + CO_3^{2-} \longrightarrow [Ru(bpy)_2(CO)(\eta^1\text{-}CO_2)] + CO_2 \quad (8)$$

Thus, the reaction of Eq. 8 is the first example of the oxide transfer from CO_3^{2-} to M–CO, and the resultant [Ru(bpy)$_2$(CO)(η^1-CO_2)] remained unchanged even after CO_2 bubbling into the solution (Eq. 9).

$$[RuL_2(CO)(\eta^1\text{-}CO_2)] + CO_2 \not\rightarrow [RuL_2(CO)_2]^{2+} + CO_3^{2-} \quad (9)$$

Moreover, the reaction of [$RuL_2(^{12}CO)(^{13}CO)$]$^{2+}$ with [K(crown)]$_2{}^{12}CO_3$ evolved only $^{12}CO_2$ in CH_3CN. On the other hand, an addition of $LiCF_3SO_3$ to the CO_2-saturated CH_3CN solution containing [$RuL_2(CO)(\eta^1\text{-}CO_2)$] resulted in gradual precipitation of Li_2CO_3 with the generation of [$RuL_2(CO)_2$]$^{2+}$ (Eq. 10).

$$[Ru(bpy)_2(CO)(\eta^1\text{-}CO_2)] + CO_2 + 2Li^+ \longrightarrow [Ru(bpy)_2(CO)_2]^{2+} + Li_2CO_3 \quad (10)$$

Thus, removal of CO_3^{2-} from the solution as a precipitation forced the oxide transfer from [$RuL_2(CO)(\eta^1\text{-}CO_2)$] to CO_2 to take place in CH_3CN. The interaction of Li^+ with the η^1-CO_2 would induce the electron transfer from Ru to CO_2, which results in an increase of nucleophilicity of the CO_2 ligand to lead to the formation of CO_3^{2-}. It is worthy of note that the oxide transfer from [K(crown)]$_2CO_3$ to [$RuL_2(CO)_2$]$^{2+}$ in CH_3CN (Eq. 8) finished in a few minutes, while it took an almost one day to complete the reverse reaction in the presence of $LiCF_3SO_3$ in CO_2-saturated CH_3CN (Eq. 10).

The rate of the oxide transfer reaction from [$(CH_3)_4N]_2CO_3$ to [$RuL_2(CO)_2$]$^{2+}$ in DMSO is slow and the reaction intermediate was detected by the ^{13}C NMR spectra. The ^{13}C NMR spectra of a d_6-DMSO solution right after mixing [$RuL_2(^{12}CO)(^{13}CO)$]$(PF_6)_2$ and [$(CH_3)_4N]_2CO_3$ displayed two signals at δ=201.7 and 205.2 ppm. The chemical shifts of these signals are almost identical with those of [$RuL_2(CO)${C(O)OH}]$^+$ in DMSO, suggesting the formation of a 1 : 1 adduct by an attack of CO_3^{2-} to a carbonyl carbon of [$RuL_2(CO)_2$]$^{2+}$ (Eq. 11).

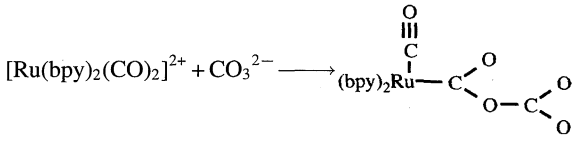

(11)

The fission of either the $RuCO_2$–CO_2 or $RuC(O)$–CO_3 bond of the 1 : 1 adduct determines the direction of the oxide transfer reactions of Eqs. 8, 9, and 10 (Scheme 1). The unusual oxide transfer reaction of Eq. 8 via the $RuC(O)O$–CO_2 bond fission (Scheme 1) is interpreted as the conversion from a weak base (CO_3^{2-}) to a weaker one ([$RuL_2(CO)(\eta^1\text{-}CO_2)$]). Although the oxide transfer reaction of Scheme 1 lies so far to [$RuL_2(CO)(\eta^1\text{-}CO_2)$], the shift to [$RuL_2(CO)_2$]$^{2+}$ in the equilibrium by an addition of Li^+ indicates the small energy difference in the formation of the two complexes.

Electrochemical Reduction of CO_2 Catalyzed by Metal Complexes

A large number of metal complexes have proven to be active as catalysts precursors in electro- and photochemical reduction of CO_2.[5] Among those metal complexes, three metal complexes: [ReCl(L)(CO)$_3$], [Ni(cyclam)]$^{2+}$ and [$RuL_2(CO)_2$]$^{2+}$, have attracted much attention because of their characteristic reactivity and high efficiency in the reduction of CO_2.

Lehn et al. reported electrochemical reduction of CO_2 catalyzed by [ReCl(L)(CO)$_3$] in 1984.[23] A series of [ReCl(L)(L′)(CO)$_2$] (L′=neutral ligand) have bifunctional ability as photosensitizers and as catalysts in the photochemical reduction of CO_2 to CO. Since they proposed a reaction mechanism for CO evolution in 1986 (Scheme 2), the arguments concerning the reaction mechanisms have still continued because no reasonable reaction intermediate has been characterized.[24] The main arguments are i) whether Cl^- or CO initially dissociates from one-electron reduced form, ii) whether another one-electron reduction takes place or not before the resultant five-coordinate (or solvated) Re complex undergoes an electrophilic attack of CO_2. A recent IR spectroelectrochemical study suggests the occurrence of the CO_2 attack to both [ReL(CO)$_3$]$^-$ (two electron reduced form) and [Re(dmbpy)(CO)$_3$]·(one electron reduced form) (dmbpy=4,4′-dimethyl-2,2′-bipyridine) depending on their stability under electrolysis conditions.[25]

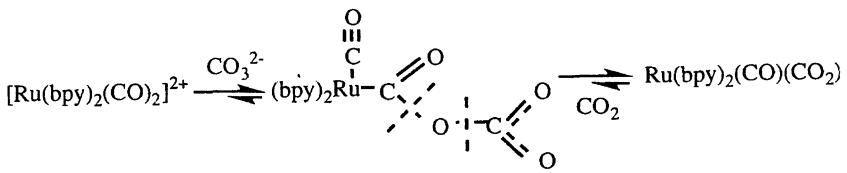

Scheme 1. The first reversible oxide transfer through a metal–C(O)–O–CO_2 adduct.

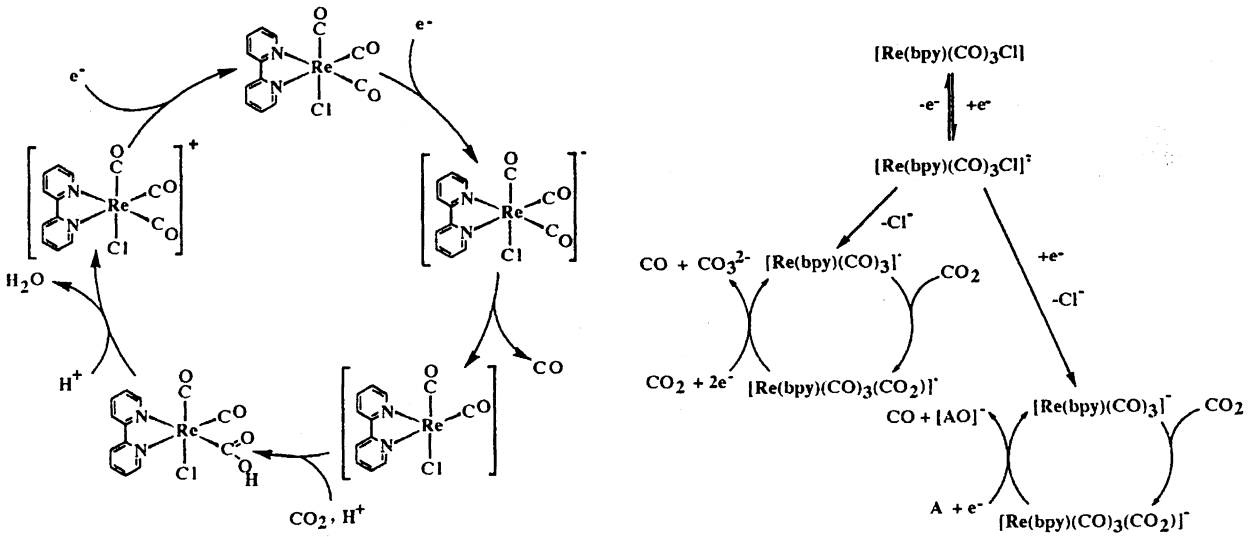

Scheme 2. Proposed mechanisms for the electrochemical reduction of CO_2 catalyzed by [Re(bpy)(CO)$_3$Cl].

Sauvage et al. found $[Ni(cyclam)]^{2+}$ adsorbed on an Hg electrode evolves CO with an almost 100% current efficiency in the electrochemical reduction of CO_2 in H_2O.[29] The reaction is explained by Scheme 3, though none of Ni–CO_2, –C(O)OH or –CO species have been identified. Sakaki et al. reported SCF ab initio calculations for $[NiF(NH_3)_4]^+$ as the model of $[Ni(cyclam)]^+$ adsorbed on Hg, and proposed a Ni^I–η^1-CO_2 adduct with the Ni–C bond distance of 1.92 Å and the OCO angle of 135.3° as the active species for the CO_2 reduction.[30] The selectivity of CO/H_2 formation in the CO_2 reduction catalyzed by Ni(macrocycle) complexes largely depends on the substituents of the ligands, and some of the derivatives are more reactive toward the selective CO_2 reduction than $[Ni(cyclam)]^{2+}$.[31] However, little is known about why $[Ni(cyclam)]^{2+}$ adsorbed on the surface of Hg selectively reduces CO_2 in H_2O via a possible intermediate of the Ni–η^1-CO_2 complex (Chart 1).

Tanaka et al. reported that electrolysis of $[RuL_2(CO)_2]^{2+}$ at −1.20 V (vs. SCE) in DMF/H_2O (1 : 9 v/v, pH 6.0) under CO_2 atmosphere produced CO and H_2, while the same electrolysis conducted at pH 9.5 gave H_2, CO, and $HCOO^-$ with a mole ratio of 1 : 1 : 1 in 1985.[26] Furthermore, the electrochemical reduction of CO_2 by $[RuL_2(CO)_2]^{2+}$ in dry CH_3CN in the presence of Me_3NHCl as a proton source predominantly produces $HCOO^-$ with a current efficiency of 85%.[27] The alternation of the main product from CO to $HCOO^-$ with decreasing the proton concentrations in the reaction media is correlated with the equilibrium among $[RuL_2(CO)_2]^{2+}$, $[RuL_2(CO)\{C(O)OH\}]^+$ and $[RuL_2(CO)(\eta^1\text{-}CO_2)]^0$ (Eq. 4) in the solution. Moreover, photochemical reduction of CO_2 catalyzed by the $[RuL_2(CO)_2]^{2+}$/$[RuL_3]^{2+}$/$N(CH_2OH)_3$ system in dry DMF selectively produces $HCOO^-$ in a quantum yield (η=14%), while CO becomes the main product (η=14.8%) in the similar CO_2 reduction catalyzed by the $[RuL_2(CO)_2]^{2+}$/$[RuL_3]^{2+}$/BNAH system (BNAH=1-benzyl-1,4-dihydronicotinamide) in DMF/H_2O mixture.[27] These facts indicate that the electro- and photochemical reductions of CO_2 catalyzed by $[RuL_2(CO)_2]^{2+}$ proceed in similar mechanisms. Electrochemical reduction of CO_2 catalyzed by

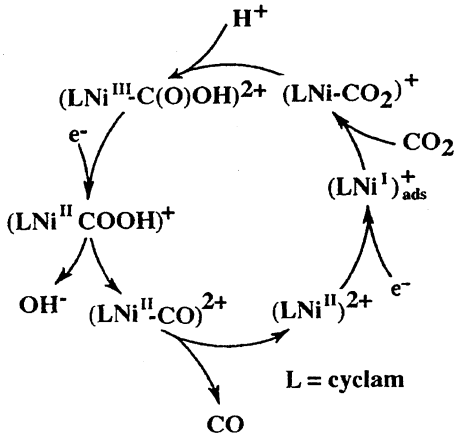

Scheme 3. Proposed mechanism for the electrochemical reduction of CO_2 by $[Ni(cyclam)]^{2+}$.

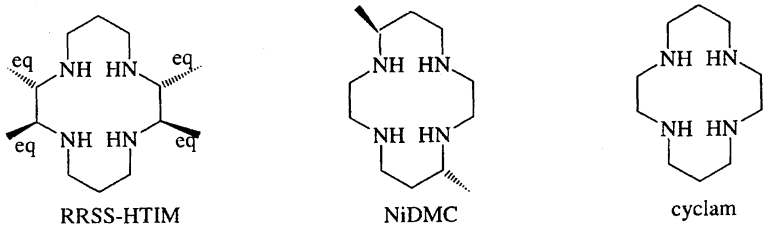

RRSS-HTIM NiDMC cyclam

Chart 1. RRSS-NiHTIM^{2+}, NiDMC^{2+}, and Nicyclam^{2+}.

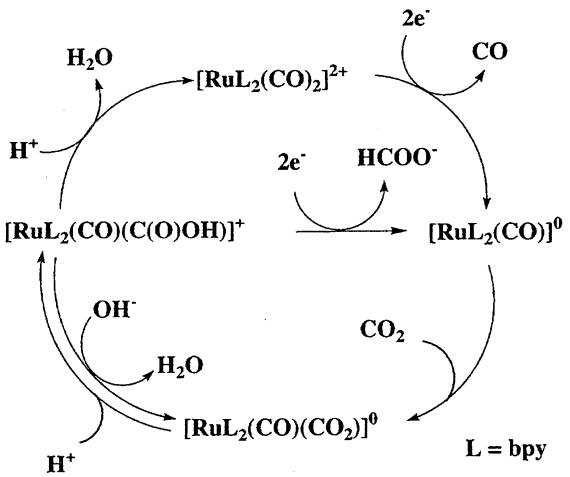

Scheme 4. Reduction of CO_2 catalyzed by $[Ru(bpy)_2(CO)_2]^{2+}$.

$[RuL_2(CO)_2]^{2+}$ is explained by Scheme 4; $[RuL_2(CO)_2]^{2+}$ undergoes irreversible two-electron reduction at -1.0 V (vs. SCE) (vide infra) to evolve CO with generating penta-coordinated $[RuL_2(CO)]^0$, which reacts with CO_2 to form $[RuL_2(CO)(\eta^1\text{-}CO_2)]$. Protonation of $[RuL_2(CO)(\eta^1\text{-}CO_2)]$ gives $[RuL_2(CO)_2]^{2+}$ through $[RuL_2(CO)\{C(O)OH\}]^+$, both of which function as the precursors to CO and $HCOO^-$ formation. It is worthy of note that $[RuL_2(CO)(\eta^1\text{-}CO_2)]$ is stable in CH_3OH as expected from the pK_a value of 9.6, but the $\eta^1\text{-}CO_2$ complex is completely protonated to give $[RuL_2(CO)\{C(O)OH\}]^+$ under CO_2 in the same solvent due to the exothermic formation of $CH_3OCO_2^-$ (Eq. 12).

$$[Ru(bpy)_2(CO)(\eta^1\text{-}CO_2)] + CH_3OH + CO_2 \longrightarrow [Ru(bpy)_2(CO)\{C(O)OH\}]^+ + CH_3OCO_2^- \quad (12)$$

The complete protonation of $[Ru(bpy)_2(CO)(\eta^1\text{-}CO_2)]$ affording $[Ru(bpy)_2(CO)\{C(O)OH\}]^+$ in CH_3OH under CO_2 (Eq. 12) is, therefore, responsible for the predominant formation of $HCOO^-$ in the photo- and electrochemical reduction of CO_2 in the presence of weak proton donors. Besides $[RuL_2(CO)\{C(O)OH\}]^+$ derived from the equilibrium of Eq. 4, $[RuL_2(CO)\{OC(O)H\}]$ resulting from CO_2 insertion into the Ru–H bond of $[RuL_2(CO)H]^0$ is also suggested as a precursor to $HCOO^-$ in the reduction of CO_2 catalyzed by $[RuL_2(CO)_2]^{2+}$.[28] Although an intramolecular rearrangement from $[RuL_2(CO)\{OC(O)H\}]^+$ to $[RuL_2(CO)\{C(O)OH\}]^+$ to explain CO evolution has been also proposed, the conversion between M–OC(O)H and M–C(O)OH has not been demonstrated so far.

Multi-Electron Reduction of CO_2 under Protic Conditions

Electro- and photochemical reduction of CO_2 catalyzed by metal complexes under protic conditions generates CO and/or HCOOH together with H_2. A competitive electrophilic attack of CO_2 and proton to low valent metal centers produces either M–CO_2 or M–H bonds. CO evolution is simply ascribed to a reductive cleavage of a M–CO bond resulting from the acid-base equilibrium of M–CO_2 (Eq. 2). Besides M–C(O)OH complexes, M–OC(O)H complexes derived from insertion of CO_2 into M–H bonds work as precursors to $HCOO^-$ generation. The most crucial problem in those CO_2 reductions is why multi-electron reduction of CO_2 with C–C bond formation does not take place in homogeneous reactions. It should be noticed that multi-electron reduction of CO_2 is energetically favored compared with two-electron reduction of CO_2. The standard redox potentials E^0 (vs. SCE) for CO_2 reduction shift to positive potentials (pH 7.0, 20 °C) as the number of electron involved in the reduction increases.

$$CO_2 + 2H^+ + 2e^- \rightarrow HCOOH \qquad E^0 = -0.85 \text{ V}$$
$$CO_2 + 2H^+ + 2e^- \rightarrow CO + H_2O \qquad E^0 = -0.76 \text{ V}$$
$$CO_2 + 4H^+ + 4e^- \rightarrow HCHO + H_2O \qquad E^0 = -0.72 \text{ V}$$
$$CO_2 + 6H^+ + 6e^- \rightarrow CH_3OH + H_2O \qquad E^0 = -0.62 \text{ V}$$
$$CO_2 + 8H^+ + 8e^- \rightarrow CH_4 + 2H_2O \qquad E^0 = -0.48 \text{ V}$$

Although general pathways for 4-, 6-, and 8-electron reduction of CO_2 have not been demonstrated so far, the reduction of M–CO rather than M–CO_2 is considered as the key process for multi-electron reduction of CO_2 by considering the smooth transformation between CO_2 and CO on metals. Some of the cationic metal carbonyl complexes are successively reduced to methyl derivatives through formyl-, hydroxymethyl complexes with hydride donors such as $NaBH_4$ and metal-hydrides (Scheme 5).[33] As expected from chemical reduction of M–CO to M–CH_3 (Scheme 5), reduction of M–CO to M–CHO prior to M–CO bond cleavage (CO evolution) is likely to be a key step to make the multi-electron reduction of CO_2 in the homogeneous electrochemical reduction.

There are great differences in chemical and electrochemical reductions of M–CO complexes: electrochemical reduction of $[RuL_2(CO)_2]^{2+}$ resulted in a Ru–CO bond cleavage in both protic and aprotic solutions, while a CO group of the complex is reduced to CH_3OH in a 10% yield by treatments with 4 equiv of $NaBH_4$ in CH_3CN/H_2O. Both $[RuL_2(CO)(CHO)]^+$ and $[RuL_2(CO)(CH_2OH)]^+$ were isolated as the reaction intermediates of CH_3OH in the same reaction conducted at -20 °C (Scheme 6).[34] Similarly, treatments of $[RuL(terpy)(CO)]^{2+}$ (terpy=2,2′:6′,2″-terpyridine) with 4 equiv of BH_4^- quantitatively produced CH_3OH and $[RuL(terpy)(CH_3CN)]^+$ in the same solvent, where $[RuL(terpy)$-

$$M\text{–}CO \rightarrow M\text{–}CHO \rightarrow M\text{–}CH_2OH \rightarrow M\text{–}CH_3$$

Scheme 5. Stepwise reduction of metal–CO complex.

$$[Ru(bpy)_2(CO)_2]^{2+} \xrightarrow{BH_4^-} [Ru(bpy)_2(CO)(CHO)]^+ \xrightarrow{BH_4^-/H_2O} [Ru(bpy)_2(CO)(CH_2OH)]^+ \xrightarrow{H^+} [Ru(bpy)_2(CO)(solvent)]^{2+} + CH_3OH$$

Scheme 6. Reduction of $[Ru(bpy)_2(CO)_2]^{2+}$ with $NaBH_4$.

$(CHO)]^+$ was initially formed in the same reaction conducted at −40 °C. Despite the formation of $[RuL_2(CO)(CHO)]^+$ and $[RuL_2(CO)(CH_2OH)]^+$ as the precursor to CH_3OH in the reaction of $[RuL_2(CO)_2]^{2+}$ with BH_4^- (Scheme 6), electrochemical reduction of CO_2 catalyzed by the same complex produced only CO and HCOOH even at −20 °C. On the other hand, the similar CO_2 reduction catalyzed by $[RuL(terpy)(CO)](PF_6)_2$ under the same electrolysis conditions produced not only CO and $HCOO^-$ but also HC(O)H, CH_3OH, H(O)CCOOH, and $HOCH_2COOH$ (Eq. 13) (Fig. 2).

$$nCO_2 \xrightarrow[EtOH/H_2O \text{ at } -20°C]{[Ru(bpy)(terpy)(CO)]^{2+}} HCOOH + CO + HCHO + CH_3OH + HOOCCHO + HOOCCH_2OH \quad (13)$$

The difference in the catalytic activity of $[RuL(terpy)(CO)]^{2+}$ and $[RuL_2(CO)_2]^{2+}$ toward the multi-electron reduction of CO_2 is associated with the stability of the reduced forms of these complexes at that temperature. Figure 3 shows the cyclic voltammogram (CV) of both complexes in CH_3CN under N_2 and CO_2; $[RuL_2(CO)_2]^{2+}$ undergoes irreversible two-electron reduction at around −1.30 V (vs. Ag/Ag^+) at 20 and −20 °C. The CV of $[RuL(terpy)(CO)]^{2+}$ displays a reversible redox couples at $E_{1/2}=-1.37$ and an irreversible cathodic wave at −1.69 V at 20 °C, while the second redox reaction becomes a reversible electron transfer process at −20 °C. On the basis of the fact that these redox reactions takes place in polypyridyl ligands, the redox behavior of the two complexes (Fig. 3) is explained as follows: $[Ru(bpy^-)(bpy^-)(CO)_2]^0$ readily dissociates CO, while $[Ru(bpy^-)(terpy^-)(CO)]^0$ is stable at −20 °C. Moreover, the reaction

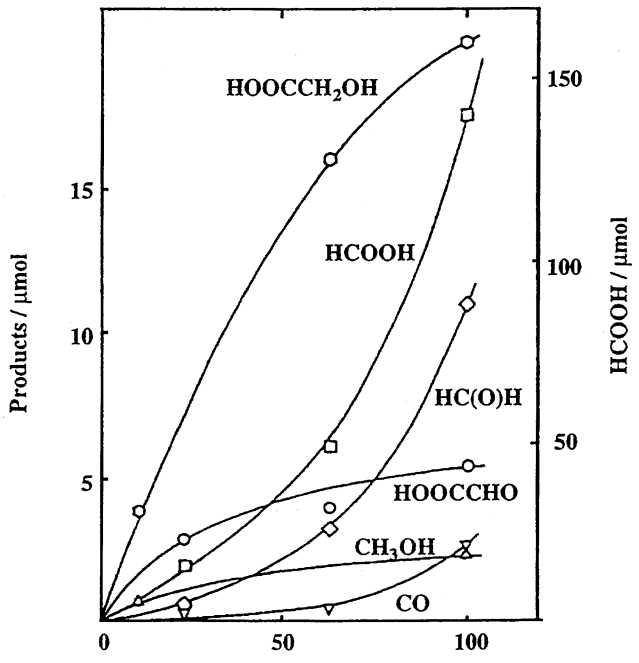

Fig. 2. Multi-electron reduction of CO_2 catalyzed by $[Ru(bpy)(terpy)(CO)]^+$ in $EtOH/H_2O$ at −20 °C.

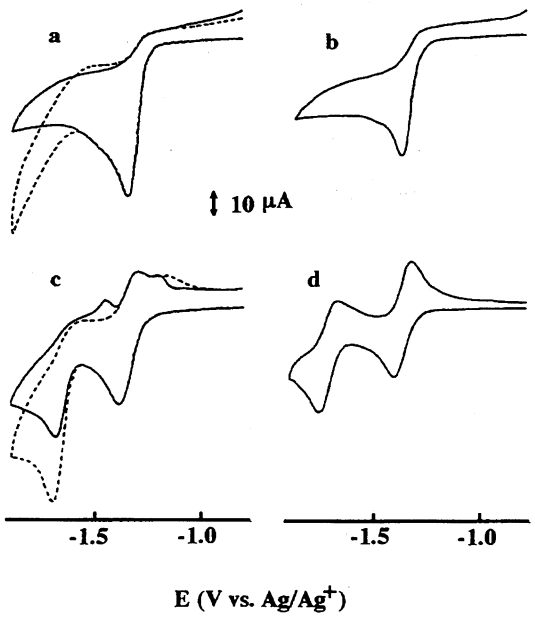

Fig. 3. Cyclic voltammograms of $[RuL_2(CO)_2](PF_6)_2$ (a and b) and $[RuL(terpy)(CO)](PF_6)_2$ (c and d) in CH_3CN at 20 °C and −20 °C under N_2 (solid lines) and CO_2 (dotted lines).

of $[RuL(terpy)(CO)]^0$ with H_2O at −30 °C produced $[RuL(terpy)(CHO)]^+$. Accordingly, the pathway for multi-electron reduction of CO_2 by $[RuL(terpy)(CO)]^{2+}$ is explained by Scheme 7. Transformation from $[RuL(terpy)(CO_2)]^0$ to $[RuL(terpy)(CO)]^{2+}$ is ascribed to the acid-base equilibrium of Eq. 2. Two-electron reduction of $[RuL(terpy)(CO)]^{2+}$ under protic conditions results in the formation of $[RuL(terpy)(CHO)]^+$ and CO evolution competitively. Protonation or carboxylation of $[RuL(terpy)(CHO)]^+$ under the electrolysis conditions gives HCHO and HOOCCHO, respectively. Further reduction and protonation of $[RuL(terpy)(CHO)]^+$ produces $[RuL(terpy)(CH_2OH)]^+$, which reacts with proton and CO_2 to generate CH_3OH and $HOOCCH_2OH$. It is, however, worthy of note that $HCOO^-$ is still formed as the main product in the CO_2 reduction (Fig. 2), even though the concentration of $[RuL(terpy)\{C(O)OH\}]^+$ must be negligibly low because of the rapid conversion from $[RuL(terpy)(\eta^1\text{-}CO_2)]$ to $[RuL(terpy)(CO)]^{2+}$ in H_2O/C_2H_5OH. A trace amount of CO evolution also reflects the smooth transformation from $[RuL(terpy)(CO_2)]^0$ to $[RuL(terpy)(CHO)]^+$ prior to CO dissociation from $[RuL(terpy)(CO)]^{2+}$ under the electrolysis conditions. Moreover, $[RuL(terpy)(CHO)]^+$, that was obtained in a stoichiometric reaction of $LiBEt_3H$ with $[RuL(terpy)(CO)](PF_6)_2$ in CD_3CN, smoothly reacts with CO_2 to produce $[RuL(terpy)(CO)]^{2+}$ and $HCOO^-$ (60% yield) even at −20 °C (Eq. 14).

$$[RuL(terpy)(CHO)]^+ + CO_2 \longrightarrow [RuL(terpy)(CO)]^{2+} + HCOO^- \quad (14)$$

Thus, $[RuL(terpy)(CHO)]^+$ is the branch intermediate for two- and multi-electron reduction of CO_2. The existence of the feedback path from thermally labile $[RuL(terpy)(CHO)]^+$ to stable $[RuL(terpy)(CO)]^{2+}$ (as the precursor for CO evo-

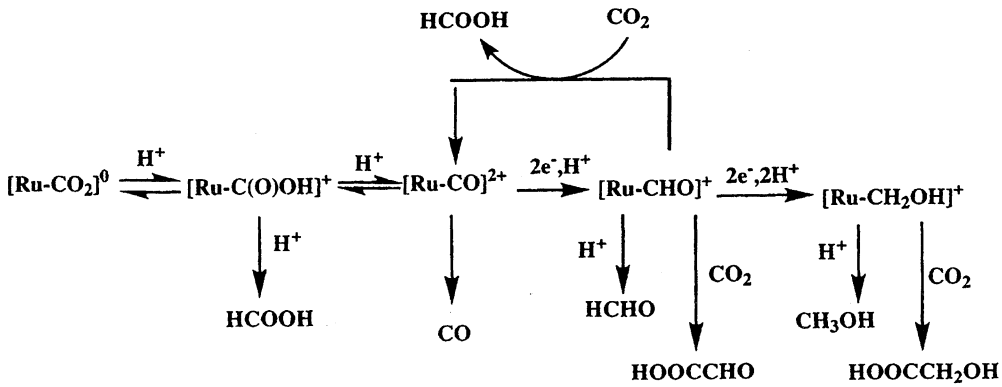

Scheme 7. Multi-electron reduction of CO_2 catalyzed by $[Ru(bpy)_2(trpy)(CO)]^+$.

lution) with generating $HCOO^-$ under CO_2 (Eq. 14) reasonably explains why only CO and/or HCOOH are produced in electro- and photochemical reduction of CO_2 catalyzed by metal complexes reported so far.[5)]

Multi-Electron Reduction of CO_2 under Aprotic Conditions

Although $[W(CO)_5(\eta^1\text{-}CO_2)]^{2-}$ and $[CpFe(CO)_2(\eta^1\text{-}CO_2)]^-$ smoothly react with CO_2 to produce $[W(CO)_6]$ and $[CpFe(CO)_3]^+$,[20a,20b)] these reactions are not suitable for reductive disproportionation reduction of CO_2 because the reduction of $W(CO)_6$ to $[W(CO)_5]^{2-}$ takes place at potentials more negative than that of the direct reduction of CO_2. The basicity of $[RuL_2(CO)(\eta^1\text{-}CO_2)]$ is not enough to undergo the oxide transfer reaction by CO_2 so that the equilibrium between $[RuL_2(CO)_2]^{2+}$ and $[RuL_2(CO)(\eta^1\text{-}CO_2)]$ lies so far to the latter under the normal conditions (Scheme 1). Replacement of a CO ligand of $[RuL_2(CO)(\eta^1\text{-}CO_2)]$ by qu (qu=quinoline) greatly enhances the basicity of the $\eta^1\text{-}CO_2$ ligand, since electrochemically prepared $[RuL_2(qu)(CH_3CN)]^0$ rapidly reacts with CO_2 to give $[RuL_2(qu)(CO)]^{2+}$ and CO_3^{2-} through $[RuL_2(qu)(\eta^1\text{-}CO_2)]$ (Eqs. 15 and 16).[35)]

$$[RuL_2(qu)(CH_3CN)]^{2+} + 2e^- + CO_2 \longrightarrow [RuL_2(qu)(\eta^1CO_2)] + CH_3CN \quad (15)$$

$$[RuL_2(qu)(\eta^1\text{-}CO_2)] + CO_2 \longrightarrow [RuL_2(qu)(CO)]^{2+} + CO_3^{2-} \quad (16)$$

Indeed, the controlled potential electrolysis of $[RuL_2(qu)(CH_3CN)]^{2+}$ (or $[RuL_2(qu)(CO)]^{2+}$) in the presence of $LiBF_4$ in CH_3CN under CO_2 at -1.40 V effectively catalyzes the reductive disproportionation of CO_2 to produce CO and CO_3^{2-} under the same electrolysis conditions (Eq. 7). On the other hand, the similar electrochemical reduction of CO_2 using $[(CH_3)_4N]BF_4$ in place of $LiBF_4$ in CH_3CN/DMSO at -1.50 V (vs. SCE) produced not only CO_3^{2-} and CO (η=42%) but also $CH_3C(O)CH_3$, $HCOO^-$ and $CH_3C(O)CH_2COO^-$ (η=16, 7, and 6%, respectively) (Eq. 17).

$$2CO_2 + 4e^- + 2(CH_3)_4N^+ \xrightarrow[-1.50\text{ V in }CH_3CN/DMSO]{[Ru(bpy)_2(qu)(CO)]^{2+}} CH_3C(O)CH_3 + CO_3^{2-} + 2(CH_3)_3N \quad (17)$$

Unexpected formation of $CH_3C(O)CH_3$ in the electrochemical CO_2 reduction results from double methylation of $[RuL_2(qu)(CO)]^0$ derived from $[RuL_2(qu)(\eta^1\text{-}CO_2)]^0$, and both $HCOO^-$ and $CH_3C(O)CH_2COO^-$ are the products in the electrochemical carboxylation of $CH_3C(O)CH_3$ catalyzed by $[RuL_2(qu)(\eta^1\text{-}CO_2)]$ (Eq. 18).

$$CH_3C(O)CH_3 + 2e^- + 2CO_2 \xrightarrow[-1.50\text{ V in }CH_3CN]{[Ru(bpy)_2(qu)(CO)]^{2+}} CH_3C(O)CH_2COO^- + HCOO^- \quad (18)$$

The rate of the formation of $CH_3C(O)CH_3$ in the electrochemical reduction of CO_2 (Eq. 17) is remarkably accelerated in the presence of CH_3I, and only $CH_3C(O)CH_3$, $HCOO^-$, and $CH_3C(O)CH_2COO^-$ were produced without evolving CO (Eq. 19).

$$2CO_2 + 4e^- + 2CH_3I \rightarrow CH_3C(O)CH_3 + CO_3^{2-} + 2I^- \quad (19)$$

The complete depression of CO evolution in these CO_2 reductions results from smooth formation of $[RuL_2(qu)\{C(O)CH_3\}]^+$ in the reaction of $[RuL_2(qu)(CO)]^0$ with CH_3I prior to the Ru–CO bond breaking (Eqs. 20 and 21).

$$[RuL_2(qu)(CO)]^0 + CH_3I \longrightarrow [RuL_2(qu)\{C(O)CH_3\}]^+ + I^- \quad (20)$$

$$[RuL_2(qu)(C(O)CH_3\}]^+ + CH_3I \longrightarrow [RuL_2(qu)(solvent)]^{2+} + CH_3C(O)CH_3 + I^- \quad (21)$$

The mechanism for the formation of $CH_3C(O)CH_3$ in the electrochemical reduction of CO_2 catalyzed by $[RuL_2(qu)(CO)]^{2+}$ is represented in Scheme 8. An electrophilic attack of CO_2 to the two-electron reduced form of $[RuL_2(qu)(solvent)]^{2+}$ produces $[RuL_2(qu)(\eta^1\text{-}CO_2)]^0$. Oxide transfer from $[RuL_2(qu)(\eta^1\text{-}CO_2)]^0$ to CO_2 generates $[RuL_2(qu)(CO)]^{2+}$ and CO_3^{2-}. Successive alkylation of $[RuL_2(qu)(CO)]^0$ by CH_3I (or Me_4N^+) gives $CH_3C(O)CH_3$. Besides the oxide transfer from $[RuL_2(qu)(CO_2)]^0$ to CO_2, the complex plays the precursor to $HCOO^-$ in the presence of $CH_3C(O)CH_3$ as a proton source, and the resultant $CH_3C(O)CH_2^-$ is trapped by CO_2 to form $CH_3C(O)CH_2COO^-$. The qu ligand effectively blocks the attack of bulky CH_3I to Ru, since neither C_2H_6 nor CH_3COO^- was formed in the reduction of CO_2 by $[RuL_2(qu)(CH_3CN)]^{2+}$. This was because the

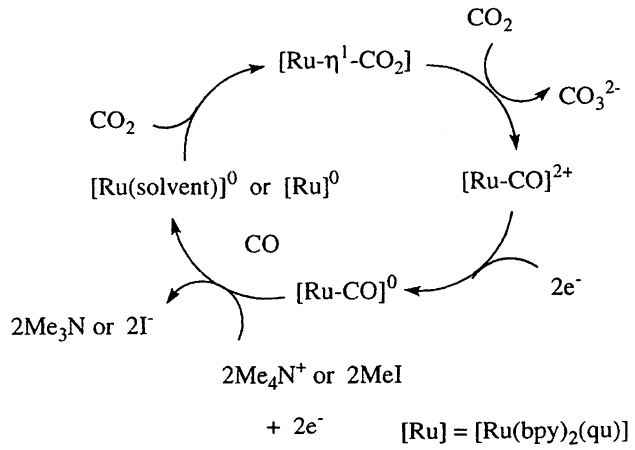

Scheme 8. Catalytic formation of acetone in electrochemical reduction of CO_2 by $[RuL_2(qu)(solvent)]^{2+}$.

electrochemical reduction of CO_2 catalyzed by $[RuL_2(L')(CH_3CH)]^{2+}$ (L′=iso−quinoline) in the presence of CH_3I produced C_2H_6, which became the main product in the similar CO_2 reduction catalyzed by $[RuL(terpy)(CO)]^{2+}$ under the similar reaction conditions.

Activation of Ru–CO Derived from Ru-η^1-CO_2

A nucleophilic attack of organic substrates to a CO group of cationic M–CO complexes is widely utilized for carbon–carbon bond formation in organic synthesis. On the other hand, an electrophilic attack of proton and CH_3I to a CO group of the two-electron reduced form of $[RuL_2(L')(CO)]^{2+}$ derived from $[RuL_2(L')(CO_2)]^0$ is the key reaction in the multi-electron reduction of CO_2 under electrolysis conditions. The efficiency of the multi-electron reduction of CO_2 accompanied by carbon–carbon bond formation, therefore, is dependent on reductive activation of not only M–CO_2 bonds but also M–CO ones. Spectroelectrochemical IR spectra greatly help to understand the reactivity of an M–CO bond depending on the oxidation states of the complexes. The ν(C≡O) band of $[RuL_2(qu)(CO)]^{2+}$ at 2015 cm^{-1} in CD_3CN undergoes the bathochromic shift to 1980 and 1939 cm^{-1} upon electrochemical one- and two-electron reductions of the complex at −1.21 and −1.50 V, respectively (Fig. 4 and Scheme 9). Thus, the ligand (bpy and qu) localized redox reaction of $[RuL_2(qu)(CO)]^{2+}$ causes the bathochromic shift of ν(CO) band by ca. 40 cm^{-1} per one electron. It is worthy of note that effective depression of CO dissociation from $[RuL_2(qu)(CO)]^0$, in contrast to $[RuL_2(CO)_2]^0$, is explained by the participation of π^* orbital of qu in the redox reaction. The ν(C≡O) band at 1980 cm^{-1} of $[RuL_2(qu)(CO)]^+$ is not affected by the presence of CH_3I, while two electron reduction of $[RuL_2(qu)(CO)]^{2+}$ in the presence of an equiv amount

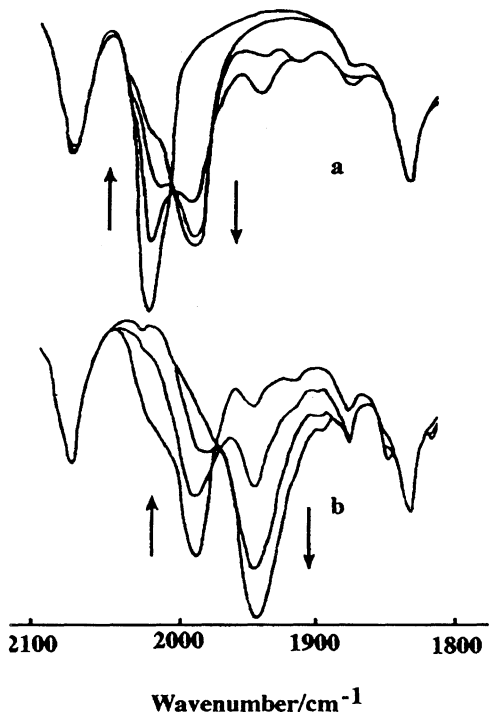

Fig. 4. Time dependent IR spectra of $[RuL_2(qu)(CO)](PF_6)_2$ under the electrolysis at −1.21 V (a) and subsequently at −1.50 V in CD_3CN containing $LiBF_4$ under N_2.

of CH_3I developed a new ν(C=O) band of $[RuL_2(qu)(C(O)CH_3)]^+$ at 1568 cm^{-1} as the precursor for $CH_3C(O)CH_3$ in the electrochemical reduction of CO_2. It is, however, not clear whether $[RuL_2(qu)(C(O)CH_3)]^+$ is formed by a direct attack of CH_3I to the CO group of $[RuL_2(qu)(CO)]^0$ or by CO insertion to a Ru–CH_3 intermediate such as $[RuL_2(qu)(CH_3)(CO)]^+$.

Intramolecular cyclization by taking advantage of a ligand localized redox reaction also greatly serves for the reductive activation of M–CO bond derived from M–CO_2. The molecular structure of $[RuL_2(napy\text{-}\varkappa N)(CO)]^{2+}$ (napy=1,8-naphthyridine) is close to that of $[RuL_2(qu)(CO)]^{2+}$. One-electron reduction of the former takes place on the napy ligand at −1.03 V (vs. Ag/AgCl). Introduction of one-electron into a π^* orbital of the monodentate napy ligand results in a remarkable enhancement of the nucleophilicity of the non-coordinated nitrogen atom. As a result, the ν(C≡O) band at 2003 cm^{-1} of $[RuL_2(napy\text{-}\varkappa N)(CO)]^{2+}$ shifted to 1585 cm^{-1} upon one-electron reduction at −1.10 V in CD_3CN. Similar one-electron reduction of $[RuL_2(napy\text{-}\varkappa N)(^{13}CO)](PF_6)_2$ also caused the red shift of the $\nu(^{13}C{\equiv}O)$ band from 1958 to 1543 cm^{-1}. The large red shift of the ν(CO) band by 418 cm^{-1} upon one-electron reduction is associated with the formation of the five-membered carbamoyl ring by an in-

$$\underset{\nu(C{\equiv}O):\ 2015}{[Ru(bpy)_2(qu)(CO)]^{2+}} \underset{-e^-}{\overset{+e^-}{\rightleftharpoons}} \underset{1980}{[Ru(bpy)_2(qu)(CO)]^{+}} \underset{-e^-}{\overset{+e^-}{\rightleftharpoons}} \underset{1939\ cm^{-1}}{[Ru(bpy)_2(qu)(CO)]^{0}}$$

Scheme 9. ν(CO) band depending on $[Ru(bpy)_2(qu)(CO)]^{n+}$ (n=0, 1, 2).

tramolecular nucleophilic attack of the non-bonded nitrogen of napy-$\varkappa$N to the carbonyl carbon (Eq. 22).[36]

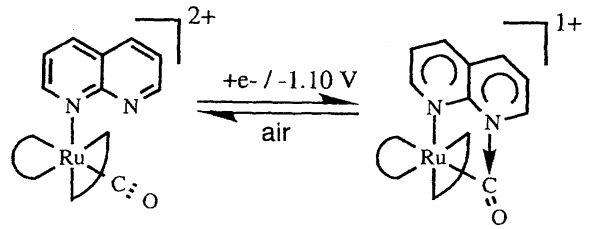

ν(C≡O) 2003 cm^{-1} ν(C=O) 1585 cm^{-1}

(22)

The rate of the $CH_3C(O)CH_3$ formation in the electrochemical reduction of CO_2 by using $(CH_3)_4N^+$ as a methylation agent is remarkably increased by participation of the five-membered carbamoyl ring (Eq. 22).

Activation of CO_2 on Non-Transition Metals

Monomeric M–η^1-CO_2 complexes may not be suitable species for CO_2 fixation to organic molecules if one considers a smooth C–O bond cleavage in protic and aprotic media. Such a C–O bond fission is practically inhibited in CO_2 bonded on organic bases. An electrophilic attack of CO_2 to O, S, and N atoms of M–XR (X=O, S) and M–NR_2 groups is usually followed by CO_2 insertion into these polarized bonds. Accordingly, μ_3-S ligands in an $M_3(\mu_3\text{-S})$ moiety may provide feasible binding sites for the activation of CO_2 without any accompanying C–O bond cleavage, because CO_2 insertion into an M–S bond of $M_3(\mu_3\text{-S})$ cores can probably be neglected due to the steric hindrance.

The pK_a values of μ_3-S of $[Fe_4(\mu_3\text{-S})_4(SC_6H_4C_nH_{2n+1})_4]^{3-}$ and $[Mo_2Fe_6(\mu_3\text{-S})_8(SEt)_3(SC_6H_4C_{2n+1})_6]^{5-}$ (n=4—12) were determined as ca. 9 and ca. 11, respectively, on the basis of the pH dependent redox reactions of $[Fe_4X_4(YC_6H_4C_nH_{2n+1})_4]^{2-}$ (X, Y=S and Se) in aqueous micellar solutions.[37] In accordance with the difference in the pK_a values, strong interaction between $[Mo_2Fe_6S_8(SEt)_9]^{5-}$ and CO_2 was confirmed in the cyclic voltammogram (CV) in dry CH_3CN, while no interaction was detected between $[Fe_4S_4(SEt)_4]^{3-}$ and CO_2 in the same solvent. Furthermore, $[Mo_2Fe_6S_8(SEt)_9]^{3-}$ catalyzes CO_2 fixation to RC(O)SEt (R=CH_3, C_2H_5, and C_6H_5) producing $RC(O)COO^-$ without evolving CO under the electrolysis at −1.50 V vs. SCE in CH_3CN (Eq. 23).[38]

$$RC(O)SEt + CO_2 + 2e^- \longrightarrow RC(O)COO^- + EtS^- \quad (23)$$

R = CH_3, C_2H_5, and C_6H_5

Catalytic formation of α-keto acids by CO_2 fixation to the carbonyl carbon of RC(O)SR′ is essentially the same reaction as the CO_2 fixation by pyruvate synthase. Based on the reactivity depending on substituents of terminal RS^- ligands, the CO_2 fixation of Eq. 23 is explained in Scheme 10: i) an electrophilic attack of CO_2 on μ_3-S of $[Mo_2Fe_6(\mu_3\text{-S})_8(SEt)_9]^{5-}$, ii) substitution of EtS^- ligated on Fe by RC(O)SEt, iii) an addition of the reductively activated CO_2 on sulfur to the carbonyl carbon of RC(O)SEt ligated on Fe. The

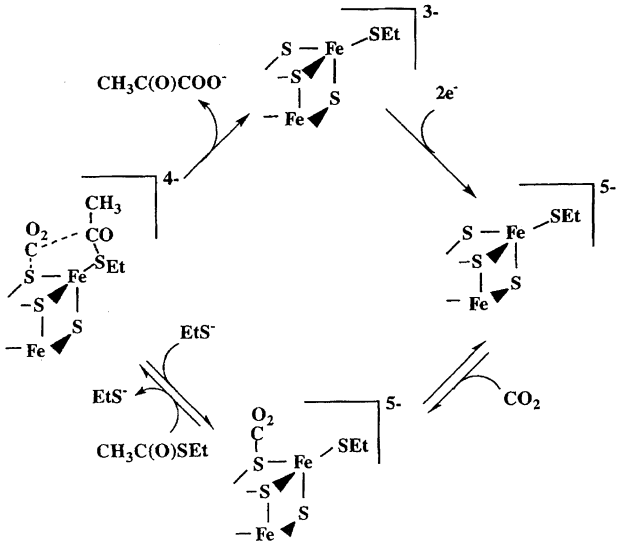

Scheme 10. Proposed path for catalytic formation of α-keto acids.

process steps i and ii are supported by the observation that an addition of free EtS^- to the solution does not block the CO_2 adduct formation with $[Mo_2Fe_6S_8(SEt)_9]^{5-}$, but strongly interferes with the α-keto acid formation due to depression of dissociation of EtS^- from Fe–SEt group.

Coupling Reaction of Two CO_2 Molecules Activated on Metal Sulfur Clusters

Oxalate formation attracts much attention from the viewpoints of carbon-carbon bond formation by one- or two-electron reduction of CO_2. Uncatalyzed electrochemical reduction of CO_2 on electrodes produces oxalate through a coupling reaction of CO_2^- (Eq. 24).

$$2CO_2 + 2e^- \xrightarrow[-2.2\ V]{} C_2O_4^{2-} \quad (24)$$

Savéant et al. have reported that anion radicals of aryl-esters and -nitrils effectively accelerate the coupling reaction of CO_2^-, though the redox potentials of those aryl compounds are quite negative and close to that of E° (CO_2/CO_2^-) at −2.21 V (vs. SCE).[39] A new route for oxalate generation without passing through free CO_2^- is, therefore, desired thermodynamically. Two-electron reduction of trinuclear metal–sulfur clusters. $[(MCp)_3(\mu_3\text{-S})_2]^{2+}$ (M=Co, Rh, Ir) causes an M–M bond cleavage in the $M_3(\mu_3\text{-S})$ core. In addition, the basicity of the μ_3-S ligand of $[(MCp)_3(\mu_3\text{-S})_2]^{2+}$ must be increased upon two-electron reduction. Two-electron reduction of $[(CpM)_3(\mu_3\text{-S})_2]^{2+}$ may, therefore, create four possible binding sites for an electrophilic attack of CO_2. The electrolysis of $[(CoCp)_3(\mu_3\text{-S})_2]^{2+}$ in CO_2-saturated dry CH_3CN at −0.70 V selectively produced $C_2O_4^{2-}$ as a white precipitate (Eq. 25).[41]

$$2CO_2 + 2e^- \xrightarrow[-0.70\ V]{[(CpCo)_3(\mu_3-S)_2]^{2+}} C_2O_4^{2-} \quad (25)$$

The oxalate formation by the reduction of CO_2 under the electrolysis at −0.7 V is particularly noteworthy since the

standard redox potential of $H_2C_2O_4$ is -0.475 V (vs. NHE) in H_2O even at pH 0 (25 °C). Similarly, oxalate was selectively produced in the electrochemical reduction of CO_2 catalyzed by $[(RhCp^*)_3(\mu_3\text{-}S)_2]^{2+}$ at -1.50 V (vs. SCE) in CH_3CN under CO_2 atmosphere.[42] In accordance with this, the two electron reduced forms of $[(CoCp)_3(\mu_3\text{-}S)_2]^{2+}$ and $[(RhCp^*)_3(\mu_3\text{-}S)_2]^{2+}$ reacted with CO_2 to produce oxalate in 80 and 60% yields, respectively, with regenerating the oxidized clusters in CH_3CN. In contrast to the reaction of $[(RhCp^*)_3(\mu_3S)_2]^0$ with CO_2 in CH_3CN, $[(IrCp^*)_3(\mu_3\text{-}S)_2]^0$ reacted with the solvent molecule under CO_2 to give $[(IrCp^*)_2(Ir(\eta^4\text{-}Cp^*CH_2CN)(\mu_3\text{-}S)_2]^+$ with a linear CH_2CN moiety bonded to a Cp^* ring (Fig. 5) and oxalate. The catalytic activity of $[(IrCp^*)_2(Ir(\eta^4\text{-}Cp^*CH_2CN)(\mu_3\text{-}S)_2]^+$ toward oxalate generation in electrochemical reduction of CO_2 is much higher than $[(CoCp)_3(\mu_3\text{-}S)_2]^{2+}$ and $[(RhCp^*)_3(\mu_3\text{-}S)_2]^{2+}$.

The IR spectra of $[(RhCp^*)_3(\mu_3\text{-}S)_2]^{2+}$ did not show any interaction with CO_2 in CD_3CN, while the electrolysis of $[(RhCp^*)_3(\mu_3\text{-}S)_2]^{2+}$ in CO_2-saturated CD_3CN at -1.50 V resulted in appearance of new bands at 1682 and 1605 cm^{-1} together with the 1633 cm^{-1} band of oxalate in the solution IR spectra. The 1680 and 1605 cm^{-1} bands completely disappeared upon the reoxidation of the solution at 0.3 V, and the 1633 cm^{-1} band of oxalate remained unchanged after the reoxidation. The 1682 and 1605 cm^{-1} bands shifted to 1636 and 1561 cm^{-1}, respectively, when the same electrolysis was conducted under $^{13}CO_2$. On the other hand, the IR spectra of $[(IrCp^*)_2(Ir(\eta^4\text{-}Cp^*CH_2CN)(\mu_3\text{-}S)_2]^+$ showed a strong peak at 1680 cm^{-1} in CO_2-saturated CD_3CN. Moreover, another band emerged around 1600 cm^{-1} upon one-electron reduction of the cluster under the electrolysis at -1.50 V in CD_3CN under $^{12}CO_2$. Prolonged electrolysis of the same solution also resulted in the appearance of the 1633 cm^{-1} band assignable to oxalate. This peak intensified with time. Thus,

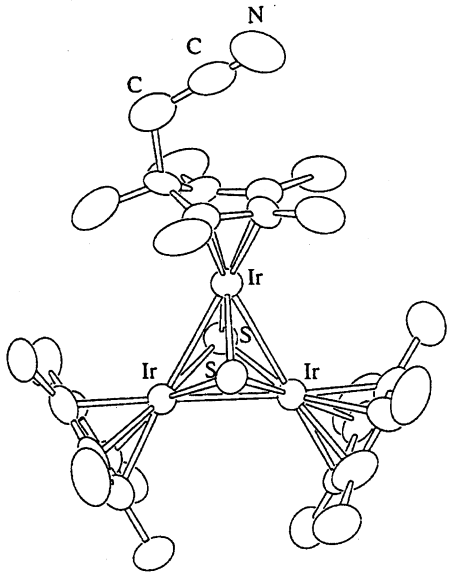

Fig. 5. Crystal structure of $[(IrCp^*)_2(IrCp^*CH_2CN)(\mu_3\text{-}S)_2]^+$ determined by X-ray analysis.

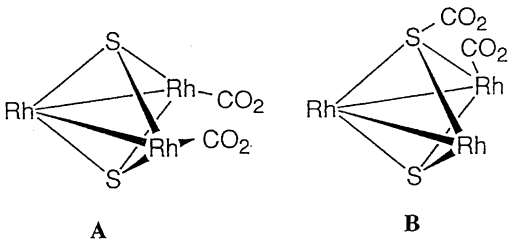

Fig. 6. Two possible structures of 1 : 2 adducts between $[(Cp^*Rh)_3(\mu_3\text{-}S)_2]^0$ and CO_2 as the precursor to $C_2O_4^{2-}$ generation.

the two $\nu(CO_2)$ bands at 1682 and 1605 cm^{-1} appeared at the same time in the IR spectra of $[(RhCp^*)_3(\mu_3\text{-}S)_2]^0$ in CD_3CN under CO_2, while the former was observed in $[(IrCp^*)_2(Ir(\eta^4\text{-}Cp^*CH_2CN)(\mu_3\text{-}S)_2]^+$ and the latter emerged in the IR spectra of $[(IrCp^*)_2(Ir(\eta^4\text{-}Cp^*CH_2CN)(\mu_3\text{-}S)_2]^0$ in CD_3CN under CO_2. These results indicate that $[(RhCp^*)_3(\mu_3\text{-}S)_2]^0$ forms a 1 : 2 adduct with CO_2 as a precursor to oxalate.

If CO_2 is linked to $[(RhCp^*)_3(\mu_3\text{-}S)_2]^0$ with an η^1-mode, the OCO angle (2α) of an adduct is expressed by Eq. 26,[43]

$$\left(\frac{\nu^i}{\nu}\right)^2 = \left(\frac{M_C}{M_C^i}\right)\left(\frac{M_C^i + 2M_O\sin^2\alpha}{M_C + 2M_O\sin^2\alpha}\right) \tag{26}$$

in which ν^i and ν represent the ν_{asym} ($^{13}CO_2$) and ν_{asym} ($^{12}CO_2$) bands (cm^{-1}), and M_C^i, M_C, and M_O are the mass number of ^{13}C, ^{12}C, and ^{16}O, respectively. On the basis of the ν_{asym} ($^{12}CO_2$) at 1682 and 1605 cm^{-1}, the OCO angles of those CO_2 molecules linked to $[(RhCp^*)_3(\mu_3\text{-}S)_2]^0$ are estimated as 157 and 132°, respectively. The latter is quite close to the OCO angle of $[Co(Pr\text{-}salen)(CO_2Na)]^+$ (135°).

There are two possibilities for the binding sites for the attack of two CO_2 molecules to $[(RhCp^*)_3(\mu_3\text{-}S)_2]^0$ (Fig. 6); one is two coordinatively unsaturated Rh atoms produced by a Rh–Rh bond fission by the two-electron reduction of the cluster and the other is Rh and μ_3-S. Ligation of two CO_2 to two Rh must be sterically blocked by bulky two Cp^* ligands (Fig. 6A). On the other hand, there seems to be no serious steric hindrance for the attack of CO_2 to μ_3-S. The appearance of a strong band at 1680 cm^{-1} in the IR spectra of $[(IrCp^*)_2(IrCp^*CH_2CN)(\mu_3\text{-}S)_2]^+$ in CO_2-saturated CD_3CN also supports an electrophilic attack of CO_2 to μ_3-S of $[(RhCp^*)_3(\mu_3\text{-}S)_2]^0$. Non-equivalence of two CO_2 molecules in the IR spectra, therefore, is explained by the attack of CO_2 molecules to Rh and S (Fig. 4B). The oxalate formation in the electrochemical reduction of CO_2 catalyzed by $[(MCp)_3(\mu_3\text{-}S)_2]^0$, therefore, is attributed to the coupling reaction of two CO_2 molecules bonded on the adjacent M and S atoms.

References

1) a) "Molecular Electrochemistry of Inorganic, Bioorganic and Organometallic Compounds," ed by C. Amatore, A. Jutand, and M. F. Nielsen, NATO ASI Ser. C (1993), 307; b) "Chemical Fixation of Carbon Dioxide," ed by M. M. Halmann, CRC Press, London (1993).

2) a) "Enzymatic and Model Carboxylation and Reduction Re-

actions for Carbon Dioxide," ed by M. Arest and J. V. Schloss, NATO Ser. C (1993); b) S. Derien, J. C. Clinet, E. Dunach, and J. Perichon, *J. Org. Chem.*, **58**, 2578 (1993); c) D. Sylvie, E. Dunach, and J. Perichon, *J. Am. Chem. Soc.*, **113**, 8447 (1991).

3) M. Aresta, C. F. Nobile, V. G. Albano, E. Fomi, and M. Manassero, *J. Chem. Soc., Chem. Commun.*, **1975**, 636.

4) a) D. H. Gibson, *Chem. Rev.*, **96**, 2063 (1996); b) J. Constamagna, G. Ferraudi, J. Canales, and J. Vergas, *Coord. Chem. Rev.*, **148**, 221 (1996).

5) a) H. Nakajima, T. Mizukawa, H. Nagao, and K. Tanaka, *Chem. Lett.*, **1995**, 251; b) K.-M. Lam, K.-Y. Wong, S.-M. Yang, and C.-M. Che, *J. Chem. Soc., Dalton Trans.*, **1995**, 1103; c) J. Costamagna, J. Canales, J. Vargas, and G. Ferraudi, *Pure Appl. Chem.*, **67**, 1045 (1995); d) A. M. Herring, B. D. Steffey, A. Miedaner, S. A. Wander, and D. L. DuBois, *Inorg. Chem.*, **34**, 1100 (1995); f) B. D. Steffey, A. Miedaner, M. L. Maciejewski-Farmer, P. R. Bernatis, A. M. Herring, V. S. Allured, V. Carperos, and D. L. DuBois, *Organometallics*, **13**, 4844 (1994); g) A. Szymaszek and F. Pruchnik, *Rhodium Express*, **5**, 18 (1994); h) E. Fujita, J. Haff, R. Sanzenbacher, and H. Elias, *Inorg. Chem.*, **33**, 4627 (1994); i) K. Ogura, H. Sugihara, J. Yano, and M. Higasa, *J. Electrochem. Soc.*, **141**, 419 (1994); j) E. Kimura, S. Wada, M. Shionoya, and Y. Okazaki, *Inorg. Chem.*, **33**, 770 (1994); k) R. J. Haines, R. E. Wittrig, and C. P. Kubiak, *Inorg. Chem.*, **33**, 4723 (1994); l) T. Ogata, Y. Yamamoto, Y. Wada, K. Murakoshi, M. Kusaba, N. Nakashima, A. Ishida, S. Takamuku, and S. Yanagida, *J. Phys. Chem.*, **99**, 11916 (1995); m) O. Ishitani, M. W. George, T. Ibusuki, F. P. A. Johnson, K. Koike, K. Nozaki, C. Pac, J. J. Turner, and J. R. Westwell, *Inorg. Chem.*, **33**, 4712 (1994), and references therein.

6) Y. Musashi, T. Hamada, and S. Sakaki, *J. Am. Chem. Soc.*, **117**, 11320 (1995).

7) a) S. Gambarotta, F. Arena, C. Floriani, and P. F. Zanazzi, *J. Am. Chem. Soc.*, **104**, 5914 (1982); b) J. C. Calabrese, T. Herskovitz, and J. B. Kinney, *J. Am. Chem. Soc.*, **105**, 5914 (1983).

8) a) D. A. Gangi and R. R. Durand, Jr., *J. Chem. Soc., Chem. Commun.*, **1986**, 697; b) D. J. Pearce and D. Pletcher, *J. Electroanal. Chem.*, **197**, 317 (1986); c) M. H. Schmidt, G. M. Miskelly, and N. S. Lewis, *J. Am. Chem. Soc.*, **112**, 3420 (1990); d) C. Creutz, H. A. Schwarz, J. F. Wishart, E. Fujita, and N. Sutin, *J. Am. Chem. Soc.*, **111**, 1153 (1989); e) N. Katz, D. J. Szalda, M. H. Chou, C. Creutz, and N. Sutin, *J. Am. Chem. Soc.*, **110**, 6591 (1988).

9) C. Creutz, in "Electrochemical and Electrocatalytic Reactions of Carbon Dioxide," ed by B. P. Sullivan, K. Krist, and H. E. Guard, Elsevier, Amsterdam (1993), p. 55.

10) J. M. Maher and N. J. Cooper, *J. Am. Chem. Soc.*, **102**, 7606 (1980).

11) G. R. Lee and N. J. Cooper, *Organometallics*, **4**, 794 (1985).

12) T. Herskovitz, *J. Am. Chem. Soc.*, **99**, 2391 (1977).

13) K. Tanaka, M. Morimoto, and T. Tanaka, *Chem. Lett.*, **1983**, 901.

14) D. H. Gibson and T.-S. Ong, *J. Am. Chem. Soc.*, **109**, 7191 (1987).

15) a) J. R. Sweet and W. A. G. Graham, *Organometallics*, **1**, 982 (1982); b) C. P. Casey, M. A. Andrews, and J. E. Rinz, *J. Am. Chem. Soc.*, **101**, 741 (1979).

16) K. Bowman, A. J. Deeming, and G. P. Proud, *J. Chem. Soc., Dalton Trans.*, **1985**, 857.

17) H. Tanaka, B.-C. Tzeng, H. Nagao, S.-M. Peng, and K. Tanaka, *Inorg. Chem.*, **32**, 1508 (1993).

18) K. Toyohara, H. Nagao, T. Adachi, T. Yoshida, and K. Tanaka, *Chem. Lett.*, **1996**, 27.

19) C. Amatore and J.-M. Saveant, *J. Am. Chem. Soc.*, **103**, 5021 (1981).

20) J. R. Pinkes, C. J. Masi, R. Chiulli, B. D. Steffey, and A. R. Cutler, *Inorg. Chem.*, **36**, 70 (1997).

21) H. Nakajima, K. Tsuge, and K. Tanaka, *Chem. Lett.*, **1997**, 485.

22) D. M. Kern, *J. Chem. Educ.*, **37**, 14 (1960).

23) J. Hawecker, J.-M. Lehn, and R. Ziessel, *J. Chem. Soc., Chem. Commun.*, **1984**, 328.

24) a) i B. P. Sullivan, C. M. Bolinger, D. Conrad, W. J. Vining, and T. J. Meyer, *J. Chem. Soc., Chem. Commun.*, **1985**, 1414; b) T. R. O'Toole, B. P. Sulliva, M. R. -M. Bruice, L. Margerum, R. W. Murray, and T. J. Meyer, *J. Electroanal. Chem.*, **217**, 259 (1989); c) P. Christensen, A. Hamnett, A. V. G. Muir, and J. A. Timney, *J. Chem. Soc., Dalton Trans.*, **1992**, 1455.

25) F. P. A. Johnson, M. W. George, F. Hartl, and J. J. Turner, *Organometallics*, **15**, 3374 (1996).

26) a) H. Ishida, K. Tanaka, and T. Yanaka, *Organometallics*, **6**, 181 (1987); b) H. Ishida, H. Tanaka, K. Tanaka, and T. Tanaka, *J. Chem. Soc., Chem. Commun.*, **1987**, 131.

27) H. Ishida, K. Tanaka, and T. Tanaka, *Inorg. Chem.*, **6**, 553 (1987).

28) J. R. Pugh, M. R. M. Bruice, B. P. Sullivan, and T. J. Meyer, *Inorg. Chem.*, **30**, 86 (1991).

29) M. Beley, J.-P. Collin, R. Ruppert, and J.-P. Sauvage, *J. Am. Chem. Soc.*, **106**, 7461 (1986).

30) a) S. Sakaki, *J. Am. Chem. Soc.*, **112**, 7813 (1990); b) **114**, 2055 (1992).

31) E. Fujita, J. Haff, R. Sanzenbacher, and H. Elias, *Inorg. Chem.*, **33**, 4627 (1994).

32) S. Chardon-Noblat, M.-N. Collomb-Dunand-Sauthier, A. Deronzier, R. Ziessel, and D. Zsoldos, *Inorg. Chem.*, **33**, 4410 (1994).

33) a) P. M. Treichel and R. L. Schubhin, *Inorg. Chem.*, **6**, 1328 (1967); b) C. Lapinte and D. Astruc, *J. Chem. Soc., Chem. Commun.*, **1983**, 430; c) C. Lapinte, D. Catheline, and D. Astruc, *Organometallics*, **7**, 1683 (1988).

34) H. Nagao, T. Mizukawa, and K. Tanaka, *Inorg. Chem.*, **33**, 3415 (1994).

35) H. Nakajima, Y. Kushi, H. Nagao, and K. Tanaka, *Organometallics*, **14**, 5093 (1995).

36) H. Nakajima and K. Tanaka, *Chem. Lett.*, **1995**, 891.

37) a) K. Tanaka, T. Tanaka, and I. Kawafune, *Inorg. Chem.*, **23**, 516 (1984); b) K. Tanaka, and M. Moriya, and T. Tanaka, *Inorg. Chem.*, **25**, 835 (1986); c) M. Nakamoto, K. Tanaka, and T. Tanaka, *Bull. Chem. Soc. Jpn.*, **61**, 4099 (1989).

38) N. Komeda, H. Nagao, T. Matsui, G. Adachi, and K. Tanaka, *J. Am. Chem. Soc.*, **114**, 3625 (1992).

39) A. Gennaro, A. A. Isse, J.-M. Savéant, M.-G. Severin, and E. Vianello, *J. Am. Chem. Soc.*, **118**, 7190 (1996).

40) a) C. R. Pulliam, J. B. Thoden, A. M. Stacy, B. Spencer, M. H. Englert, and L. F. Dahl, *J. Am. Chem. Soc.*, **113**, 7398 (1991); b) A. Venturelli and T. B. Rauchfuss, *J. Am. Chem. Soc.*, **116**, 4824 (1994).

41) a) Y. Kushi, H. Nagao, T. Nishioka, K. Isobe, and K. Tanaka, *J. Chem. Soc., Chem. Commun.*, **1995**, 1223.

42) Y. Kushi, H. Nagao, T. Nishioka, K. Isobe, and K. Tanaka, *Chem. Lett.*, **1994**, 2175.

43) K. Nakamoto, "Infrared and Raman Spectra of Inorganic and Coordination Compounds," Wiley-Interscience Publication, New York (1986).

Koji Tanaka, Ph. D., Professor of Institute for Molecular Science: born in Osaka in 1946. He obtained his B. Sc. in Chemistry from Osaka University in 1969. After he finished his master's course in 1971, he was immediately promoted to an assistant professor in the Department of Chemistry, Faculty of Engineering, Osaka University. He received his Ph. D. for research in metal complexes with chalcogenide ligands with the late Professor Toshio Tanaka in 1975. From 1978 to 1979, he studied Fischer–Tropsch reactions with Prof. R. B. King in Georgia University. Since then, he has worked on redox reactions of bioinorganic compounds. In 1990 he was promoted to an associate professor of Osaka University, and then moved to the Institute for Molecular Science as a full professor in the same year. His current research is focused on transformation of stable small molecules driven by redox reactions of metal complexes.